

REVIEW ARTICLE

Tokamak plasma diagnosis by electrical probes

G F Matthews

JET Joint Undertaking, Abingdon, Oxon OX14 3EA, UK

Received 17 March 1994

Abstract. This paper reviews progress in the understanding and application of electrical probes for the diagnosis of tokamak edge plasmas. Langmuir probes are still one of the most commonly applied diagnostics in tokamaks but our understanding of how to interpret them in strong magnetic fields is still rather limited. Recent results from flush-mounted Langmuir probes in divertor plates are used to highlight the problem areas, in particular non-saturation of the ion current and low electron to ion saturation current ratios. The importance of measuring the parallel flow velocity in the plasma edge is highlighted and recent developments in theories for interpretation of Mach probes are discussed. Finally, the importance of diagnostics for ion temperature and impurity content is emphasized, and progress in the application of advanced electrical probes such as retarding field analysers and mass spectrometers to the tokamak boundary is reviewed in this context.

1. Introduction

The role of the tokamak edge plasma in influencing the fusion energy yield of present high- Q tokamaks is now widely recognized and is reflected in the increasing efforts devoted to the experimental and theoretical study of scrape-off layer (SOL) physics (Stangeby and McCracken 1990). Of particular concern are aspects of the plasma–surface interaction leading to impurity production and the subsequent impurity transport and contamination of the core plasma. The distributions of the charge state and energy of the ion flux incident on limiter or divertor plate surfaces are the most important factors determining the magnitude of impurity release by physical sputtering, while chemical sputtering is dependent on the constituent elements of the surface and impinging plasma (Roth 1986) and the surface temperature. The impurity transport depends strongly on the background properties of the SOL plasma, such as temperatures, densities, transport coefficients and flow velocity.

The magnitude of the sheath potential drop, V_s , between the plasma and solid surfaces in the boundary contributes substantially to the ion impact energy. Highly charged ions gain an amount of energy ZeV_s during acceleration to the surface and can be responsible for significant enhancement of the impurity source. In addition these ions add to the production of secondary electrons (Thomas 1984). The latter, together with the secondary electron yield due to incident electrons and the electron and ion temperatures, determine the value of V_s .

Langmuir probes are one of the oldest and simplest diagnostics that can be used to determine the electron temperature, floating potential, density and Mach number in the edge of a tokamak. Unfortunately, the relative ease with which one can apply

a voltage to a probe element and measure a current is offset by serious issues of interpretation. There is still no entirely satisfactory theory for Langmuir probes in strongly magnetized plasmas. Fortunately, however, there is a significant body of experimental evidence that a simple interpretation yields results consistent with other diagnostics in many circumstances.

Information about the plasma ions can be obtained with more complicated probes. Passive surface collection techniques have been used to infer the impurity ion temperature (Cohen 1978, Staudenmaier *et al* 1980, Sofield *et al* 1981) and even the charge state distribution (Pitts *et al* 1989), but the methods are slow and inaccurate. Measurements of the impurity spectral emission from the plasma edge have been used to estimate the local ion temperature (McCracken *et al* 1990, Stamp and Summers 1990), but such methods do not directly measure the ion energy distribution and are necessarily averaged over some volume of plasma. Spectroscopic evaluation of the charge state distribution is also possible (Behringer 1987), although the local electron temperature in the emission zone must be known for calculation of photon efficiencies. Uncertainties in the atomic physics of many spectral lines in low-temperature plasmas with high neutral densities can also make this approach difficult. Change exchange spectroscopy with a diagnostic neutral beam can measure ion temperature and density (Schorn *et al* 1991, 1992, von Hellermann and Summers 1993). However, one is usually restricted to probing the higher charge states. Advanced electrical probes such as retarding field analysers and mass spectrometers together have the capability to provide an almost complete picture of the ion energy, charge state distribution and even secondary-electron emission yields for ions arriving at a surface in the SOL (Matthews *et al* 1991a). These measurements can test the predictions of impurity transport codes such as LIM (Stangeby *et al* 1988).

The purpose of this paper is to review progress in the application of electrical probes to the diagnosis of the plasma boundary in tokamaks. It aims to bring up to date important issues relating to the application and interpretation of Langmuir probes since the review by Stangeby (1989) and also to review developments in advanced electrical probe techniques which have occurred since the review by Manos and McCracken (1986). The application of electrical probes to fluctuation measurements is a topic deserving of a review in itself and is beyond the scope of this paper.

2. Langmuir probes

To test physics contained within the edge plasma codes we ideally need to measure all relevant plasma parameters at every point within the SOL. Langmuir probe data on their own can be used to test the predictions of edge fluid codes regarding the relationship between electron temperature and density at the divertor targets and in the SOL. Figure 1 shows an example from JET in which measurements made with a fast-moving probe in the main plasma are compared with probe measurements taken at the target plate (Vlases *et al* 1992), the prediction of the EDGE1D fluid code are also shown and are in good agreement.

Langmuir probes remain the most reported edge diagnostic in the tokamak literature, primarily because it is relatively easy to measure the voltage-current characteristics of an object inserted into a plasma. Reviews of the theoretical and

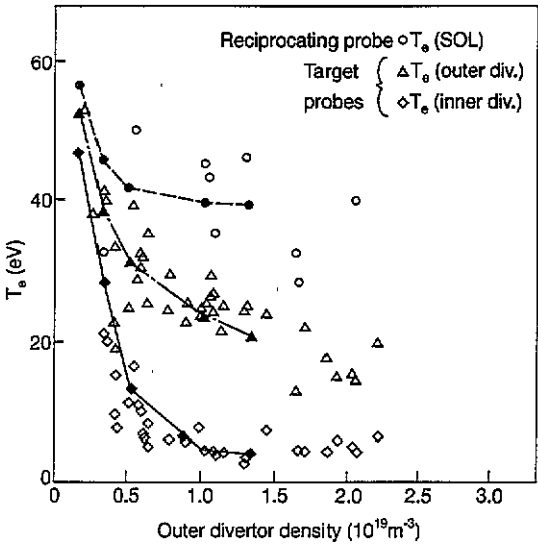


Figure 1. Comparison of T_e measured with a reciprocating Langmuir probe in the SOL of JET near the stagnation point with that measured with fixed probes located in the divertor targets. Full curves show predictions of the EDGE1D fluid code.

experimental basis for interpretation of Langmuir probes have recently been carried out for fusion (Stangeby 1989) and non-fusion applications (Hershkowitz 1989). From these references it can be concluded that Langmuir probes suffer from the first law of diagnostics—the ease of interpretation is inversely proportional to the ease of implementation. Figure 2 shows a typical Langmuir characteristic from the SOL of T10 (Gunther *et al* 1990). A conventional analysis of such characteristics involves fitting the data up to the voltage at which electron current saturates with the standard Langmuir formula

$$I = I_{is}[1 - \exp(V - V_f)/T_e] \quad (1)$$

where I is the current drawn by the probe at applied voltage V . The three free parameters in this fit are the ion saturation current (I_{is}), electron temperature (T_e) and floating potential (V_f) of the probe. Ideally this fit would include all the data up

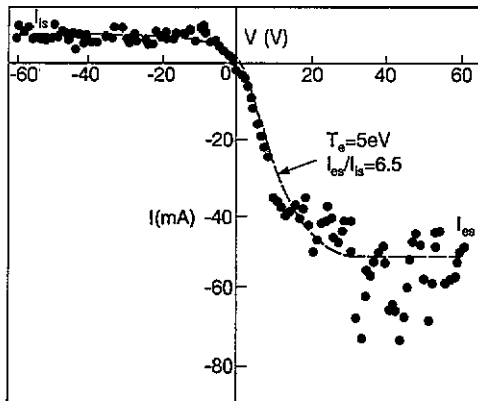


Figure 2. Langmuir probe characteristic recorded in T10 showing low electron to ion saturation current ratio.

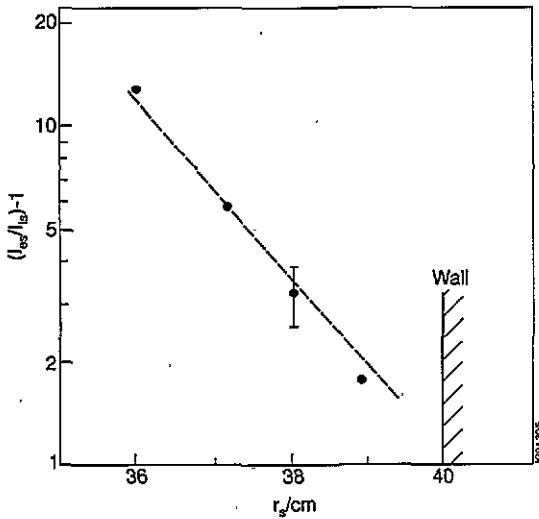


Figure 3. Radial variation of electron to ion saturation current ratio in T10.

to the point in the characteristic where electron saturation occurs. In the absence of a magnetic field the ratio between the electron and ion saturation currents $R_{ei} = I_{es}/I_{is}$ should be around 50 but in tokamaks it is found to be much lower, as can be seen from figure 2 (Gunther *et al* 1990). It has also become apparent that when the angle between the magnetic field and the surface is small the ion current does not saturate.

2.1. Electron to ion saturation current ratio

Figure 3 shows the considerable radial variation of the electron to ion saturation current ratio in T10 (Gunther *et al* 1990). Since we do not use the electron saturation current for determining T_e or n_e then it is not obvious that this has a problem. However, it has also been found that the characteristic deviates from the simple exponential for bias potentials above floating potential. In JET it was shown that the electron current increases more slowly above the floating potential than is expected. This means that as more points are included in a conventional fitting procedure from the electron side of the characteristic, the higher the derived electron temperature, as shown in figure 4 (Tagle *et al* 1987). In practice when dealing with noisy data some points often have to be included from the electron side since the statistical errors would otherwise dominate. This non-ideal behaviour of net electron collection was explained using a model developed by Stangeby (1982) in which the electron flow to the probe is restricted by momentum loss to the ions. Below floating potential when net ion current is being collected the momentum loss to the electrons can be ignored. Hence, if we restrict ourselves to fitting the characteristic below the floating potential we can use the conventional Langmuir theory to extract a value for T_e . The disadvantage of this is that we are basing our electron temperature measurements on about 5% of the electron distribution function, that of the high-energy tail.

Stangeby computes the effect of the loss of parallel electron momentum by

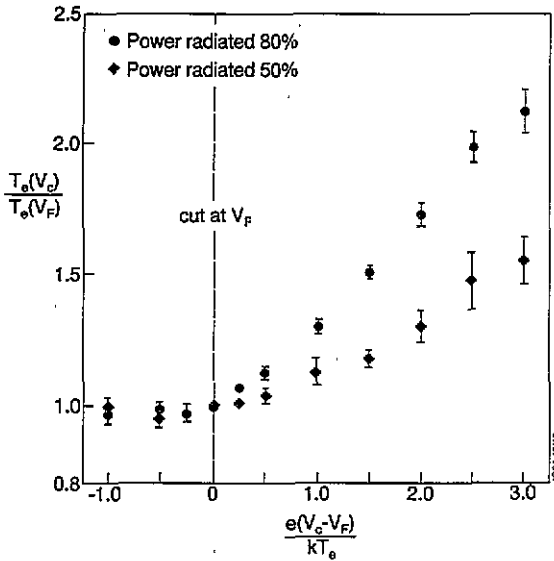


Figure 4. Variation of inferred T_e with normalized cut-off voltage. Raw probe data was obtained on JET with a single Langmuir probe of area 0.5 cm^2 . Inferred T_e rises as more points from the electron collection side of the characteristic are included. The distortion in the characteristics appears to be greater in strongly radiating plasmas.

introducing the electron mobility and relating it to the parallel diffusivity using the Einstein relation

$$\frac{D_{\parallel}^{-}}{\mu_{\parallel}^{-}} = -\frac{kT_e}{e} \quad (2)$$

The parallel electron flux is given by

$$\Gamma_{\parallel}^{-} = -D_{\parallel}^{-} \frac{dn}{dx} + n\mu_{\parallel}^{-} E \quad (3)$$

which seems reasonable since parallel transport is expected to be classical. Unfortunately, the cross-field transport cannot be ignored since it determines the extent of the electron collection region along the magnetic field L_{col}^{-} . Stangeby makes the convenient assumption that the cross-field electron flux is governed by a similar equation to the parallel electron flux with the cross-field mobility μ_{\perp}^{-} defined again via the Einstein relation but with an anomalous cross-field diffusion coefficient D_{\perp}^{-} . Attempts have been made to fit the observed reductions in electron saturation current to the model and thereby extract values for D_{\perp}^{-} (Budny and Manos 1984, Tagle *et al* 1987). However, since there is no physical basis for the assumptions made in the model, this exercise is rather pointless.

The mechanism by which current is drawn across the magnetic field must in reality be rather complicated since the electric field required to draw the current will cause ions and electrons to undergo $\mathbf{E} \times \mathbf{B}$ drifts as shown in figure 5(a). In an infinite non-viscous plasma the ions and electrons will rotate around the flux tube connecting with the probe element and no current will be drawn. Gunther (Gunther *et al* 1990) has developed a solution to this problem including the role of viscosity. However, although more rigorous his analysis assumes that the viscous forces are generated by cold recycled neutrals which are re-ionized on the same flux tube.

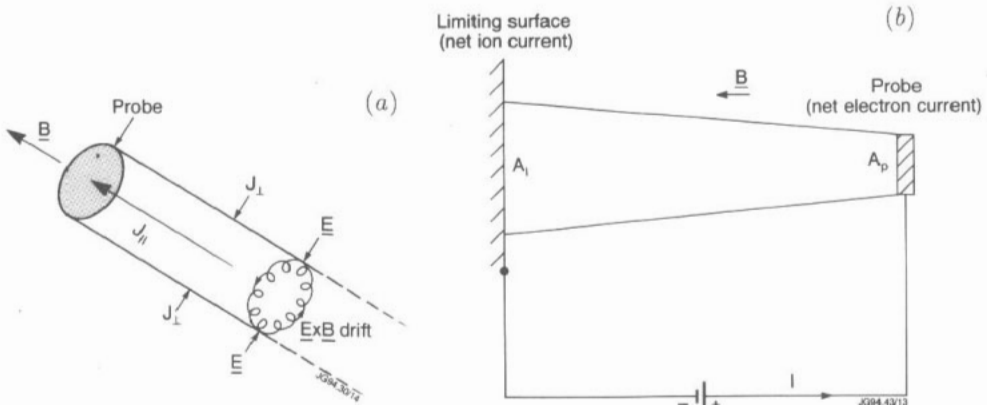


Figure 5. (a) In infinite non-viscous magnetized plasmas there is no mechanism for drawing a cross-field current. Ions and electrons would merely undergo $E \times B$ drifts around the probe axis. Gunther has included the effects of viscosity in calculating the electron collection length (b) In electron collection Gunther predicts that the collection region is so long that it will normally connect with a limiting surface and therefore behave like a double probe.

A quantitative theory of this type will always hit the problem that cross-field viscosity is not yet understood. Given that the relationship between χ_{\perp} and D_{\perp} is not classical it seems reasonable to expect that the relationship between D_{\perp} and η_{\perp} will also be anomalous.

Both the Stangeby and Gunther models make predictions for the ratio between the parallel collection lengths for ions (L_{\parallel}) and electrons (L_{\parallel}^{-})

$$L_{\parallel} = \frac{c_s d^2}{D_{\perp}} \tag{4}$$

where c_s is the ion acoustic speed and d the probe width, and the collection length for electrons is L_{\parallel}^{-} . Stangeby's model gives

$$\frac{L_{\parallel}^{-}}{L_{\parallel}} \approx 4 \times 10^6 \frac{D_{\perp} T_e^{3/4}}{d \sqrt{D_{\perp}^{-} n_e}}. \tag{5}$$

For typical SOL parameters $n_e = 10^{19} \text{ m}^{-3}$, $T_e = 25 \text{ eV}$, $d = 5 \times 10^{-3} \text{ mm}$ and $D_{\perp} = 0.5 \text{ m}^2 \text{ s}^{-1}$; the ratio $L_{\parallel}^{-}/L_{\parallel} \approx 5$ for the Stangeby model and $L_{\parallel}^{-}/L_{\parallel} \approx 100$ as determined by Gunther.

The electron collection length predicted by Gunther exceeds the parallel connection length in typical machines. This means that electron current will be drawn out of the limiting surface over a small area whose dimension depends on just how much the current channel connecting the probe tip has diffused, as shown schematically in figure 5(b). If the flux tube through which the probe has collected electrons has not expanded at all then the probe will behave like a symmetrical double probe in which current is drawn in one tip and out the other identical tip. The electron current is limited to a value equal to $A_l J_{isl}$ where A_l is the area of the footprint on the limiting surface from which electron current is drawn and J_{isl} is the ion saturation current density at the limiting surface.

Stangeby's model for low values of electron to ion saturation current ratio (R_{ei}) should be experimentally distinguishable from Gunther's. With suitable coefficients Stangeby's model can predict very low values of R_{ei} , but it does not predict the functional symmetry of the electron and ion sides of the characteristic which is characteristic of Gunther's double-probe interpretation.

2.2. Probe surface angle—the problem with grazing magnetic fields

2.2.1. *Probe types.* There are now two distinct types of Langmuir probes:

(i) probes on slow or fast (reciprocating) drives which are intended to make non-perturbing measurements of the SOL—see figure 6(a) (LaBombard *et al* 1993);

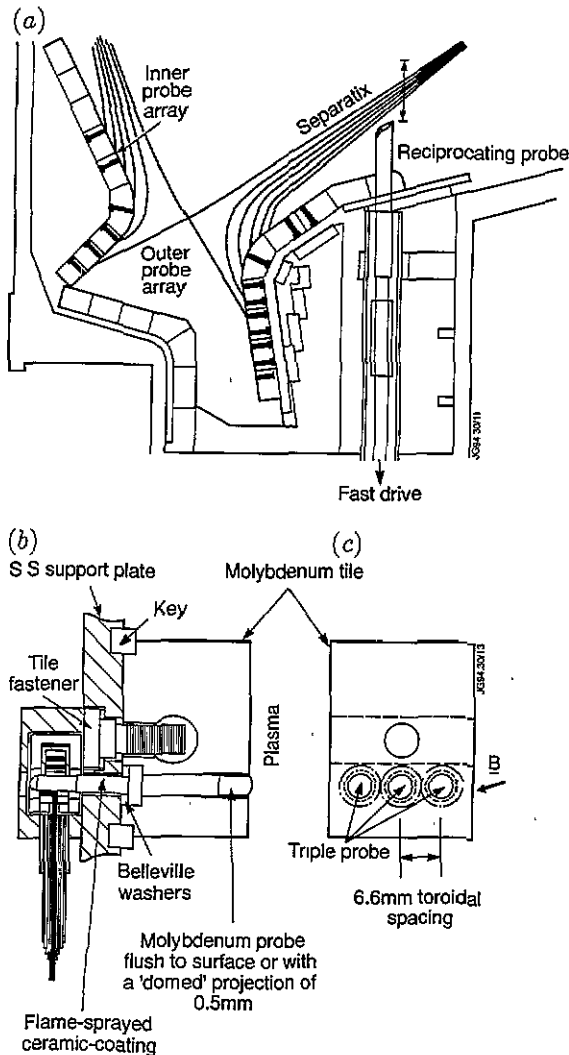


Figure 6. (a) Section through the Alcator C-Mod divertor show the fast-moving probe and target probe arrays. (b) Side view of target probes and (c) front view showing toroidal arrangement of triple probes.

(ii) Langmuir probes built into limiters and divertor targets whose purpose is to deduce plasma parameters at the plasma-surface interface—see figure 6(b) (LaBombard *et al* 1993).

Power handling problems and the need for profile determination have been solved differently in each case. The fast movable SOL probes reduce the energy deposited and obtain full profiles using movements with a duration of the order of 100 ms (Erents *et al* 1989). The probe tips are usually cylindrical pins at normal incidence to the magnetic field. In contrast, the divertor and limiter probes are fixed and have to be deployed in large numbers if full profiles are to be obtained. The JET probe design which has been adopted by DIII-D and JT60-U is similar to that used in Alcator C-Mod which is shown in figure 6(b). Such probes consist of a radiussed button which is designed to reduce the sensitivity of the projected area to magnetic field angle whilst retaining a relatively low average surface to magnetic field angle to minimize the power density.

Conventional fast probe drives are mounted on a port and are reciprocated by an external system of pneumatic pistons. Bellows provide the vacuum interface. Since ports are seldom available where they are required, the in-vessel probe drive (IVP) developed by Pitcher on ASDEX-U is likely to be adopted more widely (Pitcher *et al* 1993). This consists of a 1000-turn armature mounted on a vertical axle inside the divertor chamber is illustrated in figure 7 (Pitcher *et al* 1993). A carbon fibre reinforced arm is connected to the axle and incorporates two probe tips facing in opposite directions. When the toroidal field of the tokamak is present and current is passed through the IVP coil, $\mathbf{J} \times \mathbf{B}$ forces exert a torque on the coil which can drive the arm through 90° , and back, in a period of 150 ms. This drives the probe tips from the shelter of the baffle right across the outer leg of the divertor plasma and back again. The probes are swept at a frequency of 200 Hz.

2.2.2. *The $\sin(\theta)$ law and the funnelling effect.* It has long been assumed that because the parallel velocity of ions at a surface is around two orders of magnitude greater than the effective cross-field velocity, that the fluxes of power and particles to the surface obey a $\sin(\theta)$ law down to angles less than 1° , where θ is the grazing angle between the surface and the incident magnetic field. This law has been

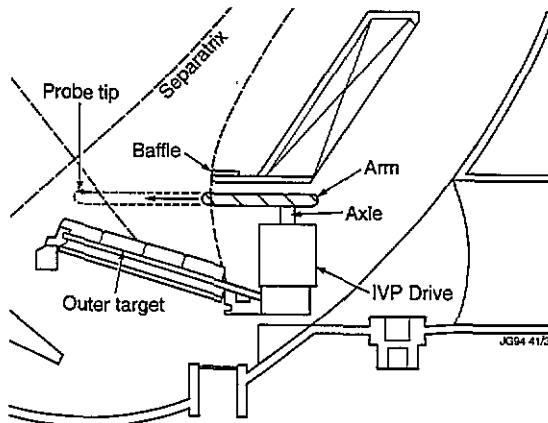


Figure 7. Schematic of the in-vessel fast probe drive on ASDEX-U.

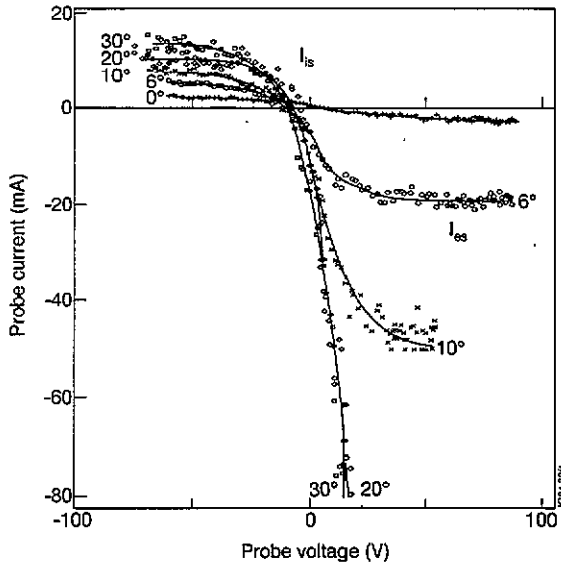


Figure 8. Probe characteristics measured on DITE with a tilting probe at various angles. When $\theta = 0^\circ$ the magnetic field lies parallel to the probe surface.

applied to the design of divertor targets, limiters and probe tips. An experimental test of this relationship was carried out in DITE (Matthews *et al* 1990) using the purpose-built array of flush-mounted Langmuir probes, and more recently in Wendelstein VII (Carlson *et al* 1993).

Examples of probe characteristics measured at various angles in DITE are shown in figure 8 (Matthews *et al* 1990a). These experiments showed that:

(i) The ion to electron saturation current ratio was a function of probe angle and typically reached unity when the tangent to the probe surface was parallel to \mathbf{B} .

(ii) The ion saturation current no longer saturated at small angles and appeared to increase linearly with voltage.

(iii) When the probe surface tangent was parallel to \mathbf{B} the ion flux was 5% of the value obtained for normal incidence. This is an order of magnitude larger than what we expect from direct cross-field deposition onto the probe surface. Evidence was also presented for anomalous cross-field deposition of power onto the TFTR 'jaws' limiter (Matthews *et al* 1990a).

This last observation was followed up by apparently contradictory infrared measurements from DIII-D (Matthews *et al* 1991b), which showed that the deposited power obeyed the $\sin(\theta)$ law down to 0.5° . These results were finally proven to be consistent by Stangeby (Stangeby *et al* 1992b) using both analytical and Monte Carlo analysis of the problem. He showed that because a probe or limiter in the scrape-off layer is a sink for plasma ions and electrons it creates a density depression which funnels particles in from closed flux surfaces; this is purely a consequence of diffusion. In the case of toroidally continuous divertor targets, the targets are not directly adjacent to the core plasma across the magnetic field and so the problem is essentially one dimensional and thus the effect is absent. The relevance of this argument to probes is that, if we were to use probes with shallow surface angles ($<10^\circ$) in both limiters and divertor plates, in the case of the limiter probes the

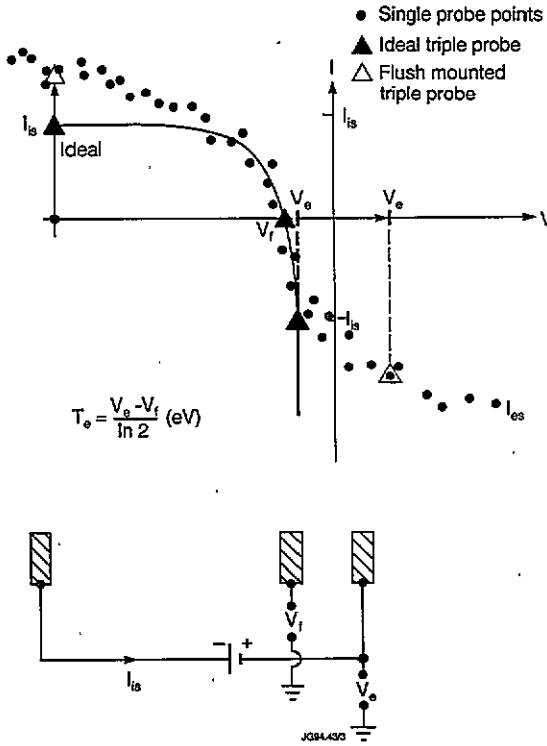


Figure 9. Principle of the triple Langmuir probe. Also indicated is the effect of non-saturation and low electron to ion saturation current ratio on the measurement.

$\sin(\theta)$ law would result in an overestimate of the electron density but not in the divertor situation (except for very grazing angles).

2.2.3. Triple probes and the consequences of small field angles. Observations (i) and (ii) in the previous section, have a serious impact on a new generation of triple-probe systems (Carlson *et al* 1993, LaBombard *et al* 1993). The principle of the triple probe is illustrated in figure 9. Three points on the probe characteristic are measured simultaneously using three separate probe tips: the ions saturation current I_{is} , the floating potential and the potential of a probe tip (V_e) drawing a current of $-I_{is}$. This analysis gives $T_e = (V_e - V_f)/\ln 2$ and is based on the assumption that the plasma is uniform across the three tips. It was demonstrated in the edge of PDX (Budny and Manos 1984) that single, double and triple probes can give very similar results. The new triple-probe systems are built into the divertor target plates and the tips are spaced toroidally to ensure plasma uniformity (see figure 6(c)) (LaBombard *et al* 1993). The systems on ASDEX Upgrade (Carlson *et al* 1993) and C-MOD (LaBombard *et al* 1993) are flush mounted to provide maximum power-handling capability. Unfortunately, this means that the magnetic field is incident on the probe surfaces at angles $< 5^\circ$ and so non-saturation of the ion current is observed. This has a direct effect on the I_{is} measured by the triple probe, but more seriously it also raises the electron current drawn by the adjacent tip. This has the effect of raising V_e and hence the apparent electron temperature as shown in figure 9.

Low values of the electron saturation current result in distortions of the electron side of the characteristic which again affects triple-probe interpretation. Non-saturation coupled with low electron saturation currents may make these probes impossible to interpret.

2.2.4. Non-saturation of ion current. If non-saturation of the ion current could be understood in terms of the parameters measured by the probe plus known geometric factors, this would solve the problems associated with flush-mounted triple probes. Alternatively, a theory might contain new parameters of interest such as the ion gyro-radius which could be introduced as a new parameter which could be extracted from the analysis of single-probe characteristics. Although much progress is being made we are still a long way from a practical solution to the problem.

Carlson (Carlson *et al* 1993) has suggested that non-saturation of ion current is caused by an extension of the sheath with voltage. Although the Debye length in the edge of current tokamaks is typically only a few tens of micrometres at most, the sheath is around 10 Debye lengths thick at floating potential and this thickness increases with probe voltage as $V^{3/4}$. The sheath thickness is comparable to the projected dimension of many flush-mounted probes. It has been shown that reasonable fits to data from flush probes in ASDEX Upgrade can be obtained with this model. However, the predicted dependence on Debye length has not been demonstrated. The angular dependence of the normalized non-saturation is predicted by the Carlson model for a flush probe and was tested in Wendelstein VII (Carlson *et al* 1993). Reasonable qualitative agreement was reported, but it does not appear good enough yet to represent a practical solution to the problem of interpreting flush-mounted triple probes.

Unfortunately, although extension of the sheath may be an important part of the story, simple models may not adequately describe real experimental data. This is because we are operating in a difficult regime where the projected dimension of the probe is comparable both to the sheath thickness and the ion gyro-radius. It is also interesting to note that the problem of non-saturation of ion current has not been reported as a problem when small cylindrical pins are used (for example Budny and Manos 1984), even though the ratio of Debye length to the projected dimensions of the pin must have been similar to that for the flush-mounted probe. This suggests that geometric factors, such as the ratio of projected area to actual surface area, may play a role; such subtlety is absent from the simple sheath extension model.

A two-dimensional kinetic model has been applied to the problem of non-saturation of the ion current and does indeed show the Child–Langmuir-type relationship $V^{3/4}$ (Bergmann 1993). This model highlights the importance of geometric details and the relative magnitudes of the Debye length, projected area and gyro-radius. In fact, at shallow angles, the scale length ratios create computational difficulties for this model.

2.3. Sheath power transmission factors—implications for probe theory

The power arriving at the divertor target can be calculated from divertor target probe data by assuming a theoretical sheath power transmission factor, or

alternatively by infrared camera measurements of the power arriving at the targets. According to the simplest model (Stangeby 1986) the power density at a surface is $P = \delta J_{sat} T_e$ where T_e is in eV, the power transmission factor (δ) is given by

$$\delta = \frac{2T_i}{T_e} + \frac{2}{1 - \gamma_e} - 0.5 \ln \left[\left(2\pi \frac{m_i}{m_e} \right) \left(1 + \frac{T_i}{T_e} \right) (1 - \gamma_e)^{-2} \right] \quad (6)$$

where γ_e is the electron secondary emission yield. Measurements on DIII-D have shown that the value of δ can vary enormously across the divertor target with the highest value near the strike point from 1–20 (Cuthbertson *et al* 1992). This result is hard to reconcile with equation (6) which on the assumption that $T_i = T_e$ gives the constant value $\delta = 7$. From the perspective of interpreting Langmuir probes this result is very worrying because two possible explanations come to mind. The first of these is that the J_{sat} recorded by the probe is not representative of the J_{sat} seen by the unbiased surface, perhaps because the effective collecting area is not simply the projected area of the probe but varies substantially as a function of local plasma conditions. High-resolution infrared measurements of a single probe tip on DIII-D show that this idea can be discounted because the power received by the tip is proportional to the projected area. A similar result can be inferred from JT60-U data in which J_{sat} is shown to be proportional to the H_α intensity over a wide range of parameters (Asakura *et al* 1993) whilst similar variations in δ similar to those in DIII-D were recorded.

The second possible explanation with implications for interpreting probes is that the variation in δ is the result of an incorrect determination of T_e . Unfortunately, this cannot be discounted and must remain a concern when it is noted that by restricting our analysis of Langmuir characteristics to the region below floating potential we are only looking at the tail of the electron distribution. This tail comprises only 5% of the total electron distribution function and so the assumption that the temperature is the same as that of the bulk is quite a bold one. Distortions in the electron distribution function can drive the apparent value of δ up or down (Stangeby 1984b).

Other possible explanations which may be considered are:

- (i) current flow across the sheath which can only increase δ (Stangeby 1986);
- (ii) secondary electron emission from the surface allows greater primary electron current to the surface which can only increase δ (Stangeby 1986);
- (iii) large ratios of T_i/T_e which can only increase δ (Stangeby 1986);
- (iv) supersonic ion flow into the sheath which can only increase δ ;
- (v) neutral collisions in the magnetic presheath have been suggested as a mechanism which could drive the value of δ down (Futch *et al* 1992) but the model seems fundamentally incapable of explaining the values of δ less than 2 which have been reported (Cuthbertson *et al* 1992).

This complex situation has yet to be resolved. Given the large number of potential explanations, it is most likely that the question of whether the T_e measured by

divertor Langmuir probes is reliable will be answered empirically by comparison with new divertor diagnostics such as Thomson scattering.

2.4. Mach probes

Measurements of the plasma flow velocity along the magnetic field in the scrape-off layer are of particular interest to tokamaks with divertors. Divertor impurity retention is governed by a delicate balance between friction with the flow of ions towards the divertor, and the ion temperature gradient force and impurity diffusion which drive the impurities out (Keilhacker *et al* 1990). Under high-recycling conditions geometric factors can result in excess ionization on a particular flux tube which exceeds the sink action of the Debye sheath at the target plate. The consequence of this is a flow-reversed layer which extends out of the divertor into the scrape-off layer (Maddison *et al* 1993). This flow can entrain impurities and drive them out of the divertor into the scrape-off layer adjacent to the core plasma where they have a much greater probability of entering the core.

So far, Mach probes have provided the only diagnostic with sufficient sensitivity and spatial resolution to study these flow patterns. The basic principle of the Mach probe is illustrated in figure 10. Two probe elements are placed back to back, sometimes with a larger separating barrier between them. In this configuration they can only receive an ion flux from one direction. It is the ratio of the ion fluxes which is used to determine the Mach number.

Stangeby (1984a) derived a simple analytical formula relating the ratio of the ion saturation currents to the Mach number of the background plasma. This derivation is essentially one-dimensional and is a variant of the standard presheath model. In the presheath an electric field is set up whose purpose is to accelerate the ions to the ion acoustic speed (Mach number $M = 1$), thus satisfying the Bohm condition at the sheath edge. This electric field depresses the electron density via the Boltzmann relation and hence the ion density, since the plasma must remain quasi-neutral. In the Mach probe model the ions a long way from the probe are assumed to have some initial velocity towards one side of the probe and away from the other. This decreases or increases the electric field required to accelerate the ions to $M = 1$ at the probe. Hence a density ratio between the two sides of the probe is predicted

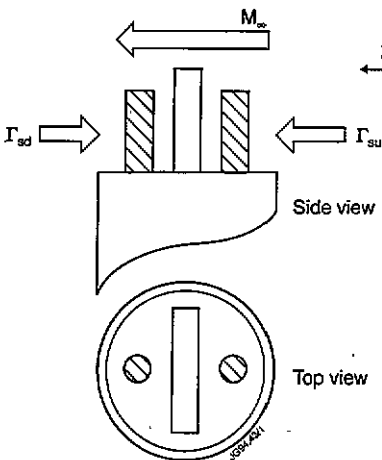


Figure 10. Schematic of a Mach probe. Ion saturation current is measured on upstream and downstream facing pins.

which is the same as the flux ratio, since the temperatures are expected to be the same on both sides of the probe.

Hutchinson has recently made considerable advances in the modelling of Mach probes. The main refinement has been to include cross-field viscosity in the analysis (Hutchinson 1988). Viscous forces acting between the flux tube connecting the probe with those to either side of it increase the current ratio by dragging ions towards the probe on one side and pushing them away at the other. Similar calculations have been extended from simple analytical approximations to two-dimensional fluid calculations (Hutchinson 1988) and a full kinetic treatment (Chung and Hutchinson 1988). It is fortunate that the additional sophistication has little impact on the results. The greatest uncertainty lies in what is assumed for the cross-field viscosity which is defined in the model by the classical relationship with an arbitrary multiplier α according to the equation

$$\eta_{\perp} = \alpha n_i m_i D_{\perp}. \quad (7)$$

When the viscosity is zero ($\alpha = 0$), Hutchinson's analytical formula for the relationship between the ion saturation current ratio (R), measured on the upstream and downstream pins, and Mach number (M) reduces to Stangeby's formula

$$M = 2 \frac{1 - R}{1 + R}. \quad (8)$$

Figure 11 shows how the current ratio depends upon α (Hutchinson 1988). At high Mach numbers the current ratio R is particularly sensitive to the value of α . This is a serious problem for the application of Mach probes because experiment shows that the relationship between χ_{\perp} and D_{\perp} is not classical and therefore the relationship

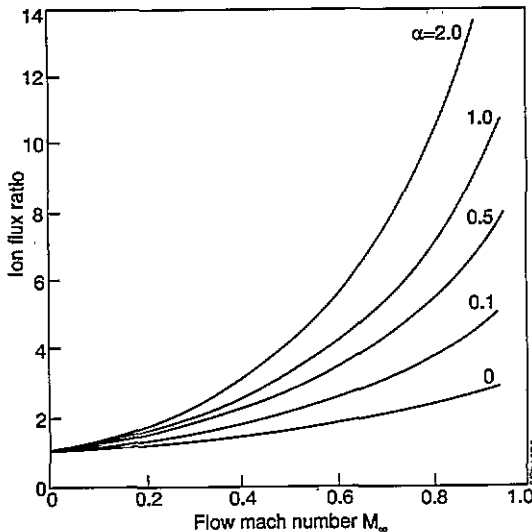


Figure 11. Hutchinson's model predicts that the relationship between Mach number and current ratio is sensitive to α particularly at high Mach numbers.

between D_{\perp} and η_{\perp} may also be anomalous. Various experimental studies have attempted to determine the value of α . The first report was from PISCES (LaBombard *et al* 1989) and attempted to distinguish between Stangeby's analytical model ($\alpha = 0$) and Hutchinson's analytical model with $\alpha = 1$; it was concluded that Stangeby's model was a better fit to the data. A more detailed study on PISCES (Chung and Hutchinson 1988) gave a best fit for $\alpha = 0.5$, indicating that viscosity can play a role.

It can be shown, with some qualification, that Hutchinson's model can be fitted with an expression of the form $R = \exp(M/M_c)$. Where R is the current ratio, M is the Mach number of the background plasma and M_c is a constant which depends on α . When $\alpha = 1$, $M_c = 0.4-0.45$ (Hutchinson 1988). Interestingly enough an identical formula had previously been obtained from a purely empirical fit to data from the DITE tokamak (Proudford *et al* 1984). In this work $M_c = 0.6$ was argued to give the most reasonable results. According to Hutchinson this corresponds to $\alpha = 0.1$. However, this cannot be claimed to be a satisfactory determination of α . It is also evident that if the relationship between η_{\perp} and D_{\perp} is not classical it would also be surprisingly good fortune if α were indeed a constant for all conditions relevant to the tokamak boundary.

The great uncertainty in the value of α means that, particularly at higher Mach numbers, Mach probes are little more than flow-direction meters. The techniques used to estimate α in PISCES would be extremely difficult to apply in a tokamak. A simpler scheme involving comparisons between connected and unconnected presheaths has recently been proposed (Chung 1993) and may lead to a practical routine diagnostic for determining α . The theory of the connected presheath has been dealt with by Hutchinson (1991) and applies to situations where the natural ion collection length of the probe exceeds the distance to the nearest material surface. However, one should be cautioned that the theory is not applicable when there are significant parallel temperature gradients and ionization sources, as is likely to be the case near a divertor target. This situation is best avoided by ensuring the probe is sufficiently small.

2.4.1. The Gundestrupp probe. The Gundestrupp probe has recently been developed at Tokamak de Varenne (TdeV) (MacLachy *et al* 1992). It consists of a circle of outward-facing planar electrodes as shown in figure 12(a). Ion saturation currents are recorded on each face to produce the type of polar plot shown in figure 12(b). This is fitted with a model which is essentially a two-component analogue of Hutchinson's one-dimensional analysis of conventional Mach probes (Hutchinson 1988); an example of such a fit is given in figure 12(b).

Although data have been presented which show a convincing correlation between the poloidal rotation measured in TdeV with a Gundestrupp probe and an imposed radial electric field (MacLachy *et al* 1992), it must be recognized that an entirely satisfactory theory for interpreting the probe has yet to be developed. This is hardly surprising given the difficulty there has been in developing a satisfactory model for conventional Mach probes which rely primarily on classical parallel transport with corrections to allow for anomalous cross-field effects. Also, the ion flux to the Gundestrupp collectors, which are at grazing angles to the field, will suffer the problems described in section 2.2.

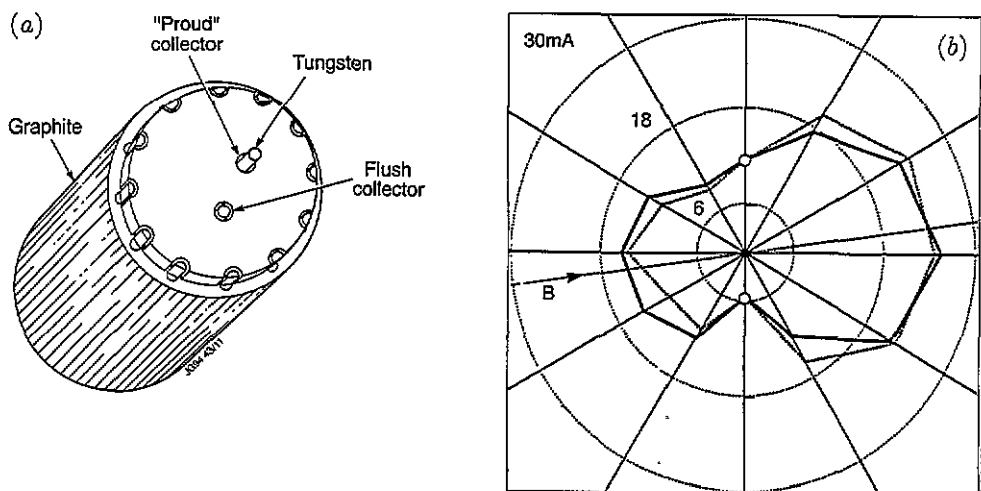


Figure 12. (a) The Gundestrupp probe developed on TdV measures ion saturation around the circumference of a cylinder. (b) Polar plots of ion saturation are fitted using a model which has $v_{||}$ and v_{\perp} as variables.

3. Ion diagnostics

3.1. The importance of ions

Recombination rates are generally very low in fusion devices and the majority of ions are lost to limiters, divertor target plates or walls via the sheath (Stangeby 1986). The impact energy of the ion on these surfaces depends on the ion temperature, the sheath voltage and charge state of ions. A conventional Langmuir probe embedded in the surface can be used to measure the ion flux and the electron temperature. As has already been described, by applying a simple probe theory, for which we must assume an ion temperature, we can extract a value for the electron density at the sheath edge and the power arriving at the surface. Using sheath theory to calculate the sheath potential we can also calculate the theoretical impact energy of the ions at the surface. However, to do this rigorously we also need to know the secondary-electron emission yield of the surface for electrons and ions, and for an impure plasma, the charge state distribution of the impinging ions.

Momentum transfer between the impinging ions and surface atoms results in physical sputtering which is the most fundamental of impurity production mechanisms (Roth 1986). Chemical sputtering occurs when chemical reactions take place between incident ions and the surface atoms producing volatile molecular products (Roth 1986). The sputtered surface atoms or molecules enter the plasma as neutrals and travel into the plasma until they are ionized. Once ionized, impurity ions are trapped by the magnetic field and are generally assumed to move parallel to the magnetic field according to classical theory (Stangeby *et al* 1988) whilst undergoing anomalous cross-field diffusion. The principle forces acting on the ions are the ion temperature gradient force and the frictional force involving the background plasma flow, and it is the balance between these forces and the diffusion process that determines whether impurities are driven away from the plate into the main plasma

or back to the plate (Keilhacker *et al* 1990). The impurity parallel diffusion coefficient (equation (8)), frictional force (equation (9)) and ion temperature gradient force (equation (10)) are strongly dependent on impurity charge state (Z_I), background ion charge state (Z_B), impurity ion temperature (T_I) and background ion temperature (T_B) as follows

$$D_{\parallel} \propto \frac{T_I^2 T_B^{0.5}}{m_B^{0.5} n_B Z_B^2 Z_I^2} \quad (8)$$

$$F_f \propto \frac{m_B^{1/2} [1 + (m_B/m_I)] n_B Z_B^2 Z_I^2 (v_B - v_I)}{T_B^{3/2}} \quad (9)$$

$$F_I \propto Z_I^2 \nabla_{\parallel} T_B \quad (10)$$

where $v_B - v_I$ is the difference in velocity between the impurities and the background plasma.

The situation is complicated by the fact that both the charge state and temperature of the impurity ions are dependent on the local density, electron and ion temperatures. Given enough information about the plasma background and a non-perturbing concentration of impurities Monte Carlo impurity transport codes, such as LIM (for tokamaks with limiters) (Stangeby *et al* 1988) and DIVIMP (for tokamaks with divertors) (Stangeby *et al* 1992a) can be used to predict the distribution and charge state mix of impurities within the plasma. Figure 13 shows a schematic of the life history of an impurity ion within the JET divertor as it might be followed by DIVIMP, from its origin as a neutral carbon atom sputtered from the divertor plate to its eventual return.

Langmuir probes on their own can tell us nothing about the ion temperature, sheath voltage or impurity content. For this reason, more sophisticated electrical probes have been developed which can give a detailed picture of impurity production and transport in the edge of a tokamak.

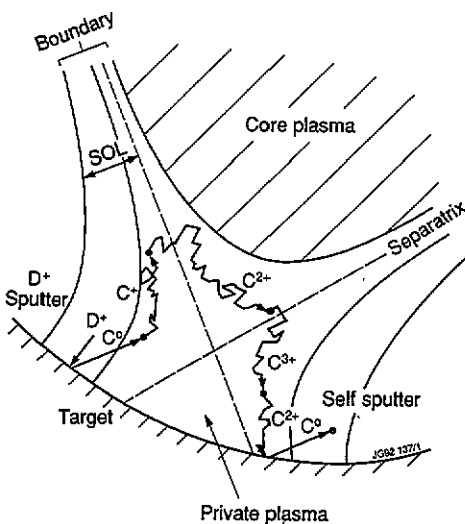


Figure 13 Schematic showing the life history of an impurity ion in a divertor plasma. A delicate force balance determines whether the impurities stay within the divertor.

3.2. Ion energy analysers

Three types of electrical ion energy analyser have been applied to diagnosing the tokamak SOL. The first and still most successful is the retarding field analyser (RFA) which applies electric fields parallel to the magnetic field. This employs a series of biasable grids, including an ion repeller grid which is swept positively, and a current collector to record the ion current. The second is the $\mathbf{E} \times \mathbf{B}$ probe which applies an electric field perpendicular to the magnetic field of the tokamak. This results in a guiding centre drift at right angles to \mathbf{B} which disperses ions across a series of collectors depending on their parallel velocity. The final technique for measuring ion temperature involves the use of plasma ion mass spectrometer (PIMS) and will be discussed in the section on mass spectrometers.

All the above devices measure parallel ion energy distributions. Apparently the only technique which is claimed to measure the perpendicular energy of the majority ions is the Katsumata probe (Katsumata and Okazaki 1967). This is essentially a recessed Langmuir probe and is shown schematically in figure 14(a) (El Shaer 1981). It is argued that electrons will not reach the probe due to their small gyro-radius and that the ions will be repelled such that if they are Maxwellian the ion current is given by $I \propto \exp[-(eV/kT_i)]$. This argument would of course be reasonable if we were dealing with an ion beam, but plasmas are by definition space-charge dominated and it is not clear exactly what will happen to the ion energy distribution if one simply strips out the electrons in this geometry. With a conventional sheath the ions are accelerated to $\sim 3T_e$ which is similar to the ion temperature we hope to observe. A code now exists which may be able to tackle the Katsumata probe problem (Bergmann 1993). However, it is not inconceivable that the result may also be influenced by the model assumed for cross-field diffusion, and if this were so interpretation would still be difficult without an adequate theory for this anomalous process. Experimental data from the Petula tokamak, shown in figure 14(b) (El Shaer 1981), shows substantial disagreement between Katsumata probe measurements and those with an RFA. The electron density in this experiment was $2 \times 10^{18} \text{ m}^{-3}$ at the probe location and the ion-ion mean free path was therefore short enough to ensure that the parallel and perpendicular ion temperatures were in equilibrium.

Techniques based on differentiating between ions with small and large ion gyro-radii do make sense in the situation where there is a small population of suprathermal ions. Manos *et al* (1982) demonstrated this technique on PLT using a recessed bolometer element which had no direct line of sight parallel to the magnetic field. Essentially, this technique measured the total power associated with suprathermal ions with gyro-radii above some threshold set by the probe geometry. Rotation of the probe head coupled with the finite acceptance angle of the probe aperture allowed some resolution of the pitch angle distribution of the incident ions. This diagnostic has some similarities to the Katsumata probe. However, since it detects only minority ions with energies considerably in excess of the sheath voltage, space-charge effects can be ignored.

To make a meaningful measurement with any ion analyser there must be a clean transition from the plasma, where electric fields are screened out over distances of order the Debye length (λ_D), to the ion beam where an analysis based on single-particle motion in vacuum fields is a good approximation. Although the sheath extends over a total distance $\approx 10\lambda_D$, there is still significant potential drop

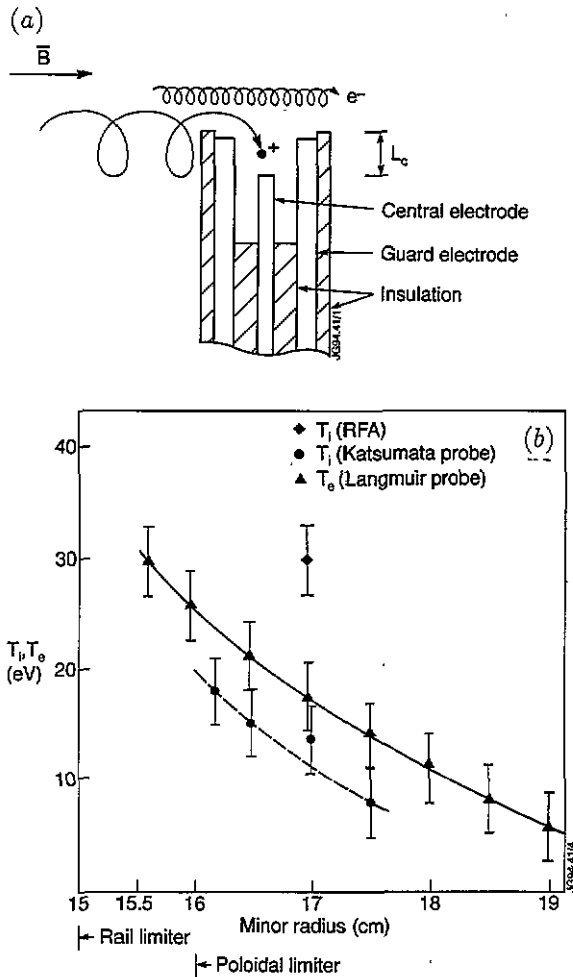


Figure 14. (a) Schematic of the Katsumata probe used in the Petula tokamak. (b) Comparison of retarding field analyser measurements with Katsumata probe measurements in Petula.

over the first Debye length. Allowing for the fact that the sheath extends from each edge of the entrance aperture a reasonable condition to work with is that the slit width should be $< 2\lambda_D$. This condition has been roughly verified experimentally on DITE (Pitts 1991a) as shown in figure 15 which shows characteristics from the same RFA with two extreme slit sizes. The first slit is of width $s = 0.005$ mm giving $s/\lambda_D = 0.18$ and the second is of width $s = 0.5$ mm giving $s/\lambda_D = 8.5$ (slits of width 0.025, 0.1 and 1 mm were also investigated). The small slit shows the sheath feature and Maxwellian decay of the ion distribution very clearly whereas the large slit shows neither of these features.

A two-dimensional kinetic treatment of the plasma is required if the problem of sampling plasmas through an aperture is to be tackled computationally. Such codes now exist (Armstrong *et al* 1992, Bergmann 1993) but have yet to be applied to this particular problem. Even if the probe aperture is sufficiently small, space charge can perturb the ion motion within the probe. Various analytical formulae can be used to

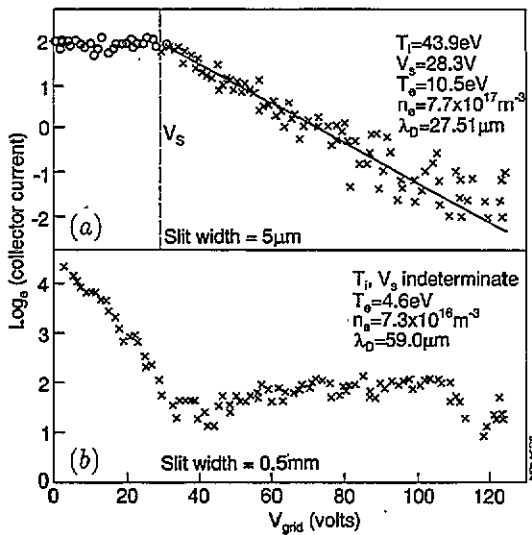


Figure 15. Comparison of RFA characteristics for the two extremes of a range of slit widths tested on DITE. (a) When $s/\lambda_D = 0.18$ there is a clear sheath feature and exponential decay. (b) When $s/\lambda_D = 8.5$ the characteristic is not even monotonic.

provide guidance (Matthews 1984a). If electrons are also present at any significant density they can partially neutralize the effects of space charge. Unfortunately, a full solution of this problem is of comparable complexity to the kinetic modelling of a plasma in more than one dimension (Armstrong *et al* 1992, Bergmann 1993). Empirical evidence, particularly from RFA experiments, is the best guide so far to the correct functioning of such devices.

3.3. Retarding field analysers

Retarding field analysers (RFAs) have been widely used in non-fusion plasmas but the high power flux and short Debye length have made it difficult to apply the technique to tokamaks (Matthews 1984a, Pitts 1991a). Grids have often been used as primary apertures (for example El Shaer, 1981) but present serious difficulties. They appear attractive because they offer the prospect of a large current which is easier to measure. However, the aperture holes in these devices have inevitably been rather large with respect to the Debye length. This is caused by the need to use a foil which is thick enough to absorb the energy deposited in a single tokamak pulse. Aperture slits can overcome this problem and provide a sub-Debye length aperture with adequate power-handling capability. Fine slits with widths down to 0.005mm are available in thin foils but such foils have a minuscule heat capacity and would rapidly melt. Two strategies have been applied to solving this problem and are illustrated in figure 16. The first is to create an aperture using knife edges ground from relatively thick material, the second is to place the thin foil containing the ultimate entrance slit behind a more robust aperture and rely on thermal conduction in the plane of the foil to keep the edges cool.

The basic principle of the RFA is illustrated by figure 17(a). Ions or electrons

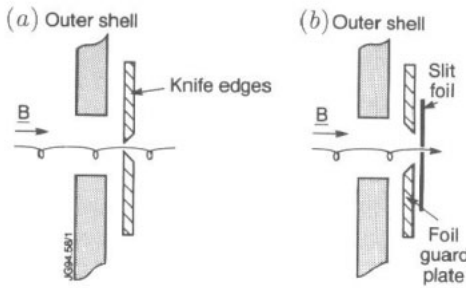


Figure 16. Slits capable of withstanding high heat fluxes can be made (a) with knife edges ground from thick material or (b) a thin foil placed in a window behind a thicker plate.

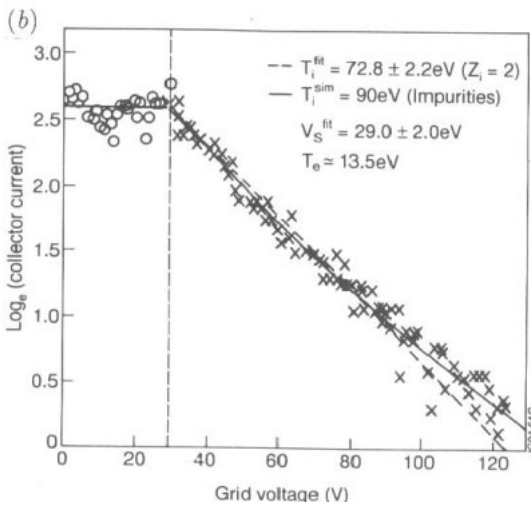
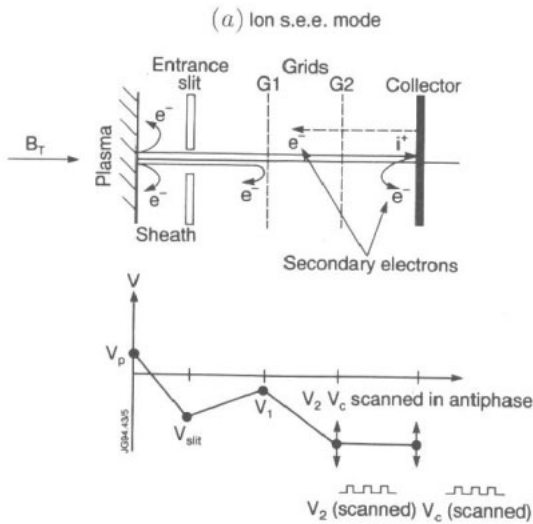


Figure 17. (a) RFA configured in the ion analysis mode. (b) RFA characteristic measured in DITE, fitted assuming a single charge state $Z = 2$ and a second fit assuming full charge state distribution measured by PIMS in a similar discharge.

can be studied depending on the bias conditions. The current–voltage characteristics which result are simply the integral of the parallel ion velocity distribution function:

$$I_c \propto \int_{\sqrt{2ZeV_{\text{grid}}/m_i}}^{\infty} v_{\parallel} f(v_{\parallel}) dv_{\parallel}$$

where V_{grid} is the voltage of the ion repeller grid. It would be nice if RFA data could be used to distinguish subtle things like the competing theories of the presheath (Pitts 1991b). However, in practice noise in the data plus the complicating effects of impurities mean that a shifted Maxwellian distribution shifted by the sheath voltage is normally assumed.

If the ion distribution function is assumed to be Maxwellian then for $V_{\text{grid}} > V_{\text{sheath}}$, $I_c \propto \exp[-(ZeV_{\text{grid}}/2kT_i)]$. By fitting these equations to the data, as shown in figure 17(b) (Matthews *et al* 1991), we can extract values for T_i/Z and V_s . Thus to obtain T_i we need to assume a value for Z . Although it might seem obvious to assume that $Z = 1$ in a hydrogenic plasma, measurements made in DITE with a plasma ion mass spectrometer (see next section) have shown that in this case $Z = 2$ is a better assumption. However, it has been shown by Pitts that even this is still an approximation (Matthews *et al* 1991) since inclusion of the full charge state distribution leads to a superposition of multiple Maxwellians. Figure 17(b) gives an example of this effect.

RFAs tend to be used for studying the ion temperature due to the paucity of other techniques. However, it is obviously possible to reverse the polarity of the grids and look at the electron distribution function using the same technique. In fact, this technique looks at the tail of the electron distribution crossing the sheath as does a conventional Langmuir probe operated below the floating potential. As shown in figure 18 (Matthews 1984a), a comparison of electron temperatures derived with an RFA with those of a Langmuir probe at the same location gives very similar results. One major difference between the two techniques is that the Langmuir probe varies the current extracted from the plasma whereas the RFA does not. This is an important test of Stangeby's Langmuir probe theory (see section 2) which

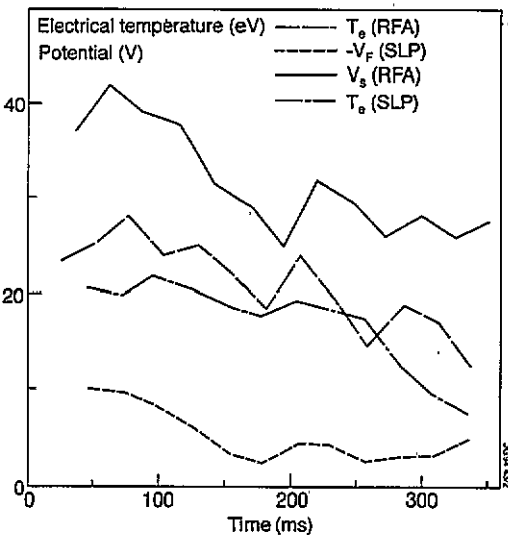


Figure 18. Comparison of electron temperature measure with a Langmuir probe and RFA in DITE.

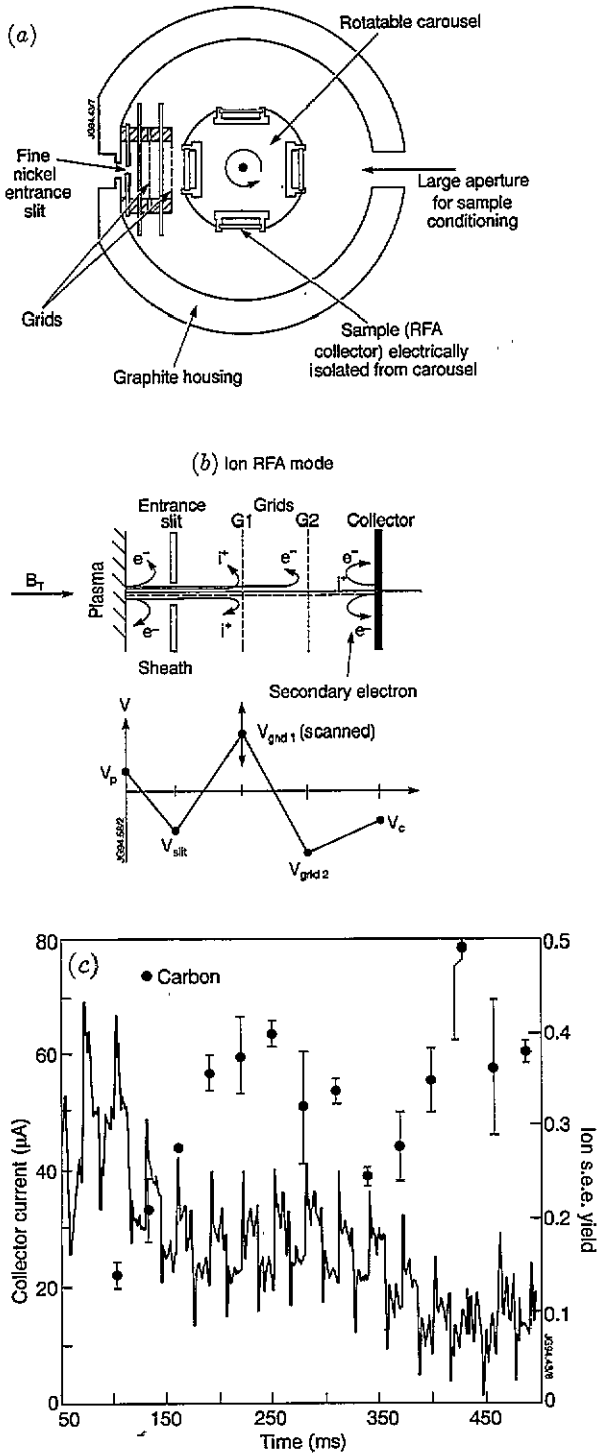


Figure 19. (a) RFA used to measure ion and electron secondary-electron yields on DITE—samples could be rotated in front of a large aperture for conditioning. (b) Bias scheme for ion-induced secondary electron mode. (c) Current versus time during ion-induced secondary electron mode for a carbon sample and the ion-induced secondary electron yield deduced from it.

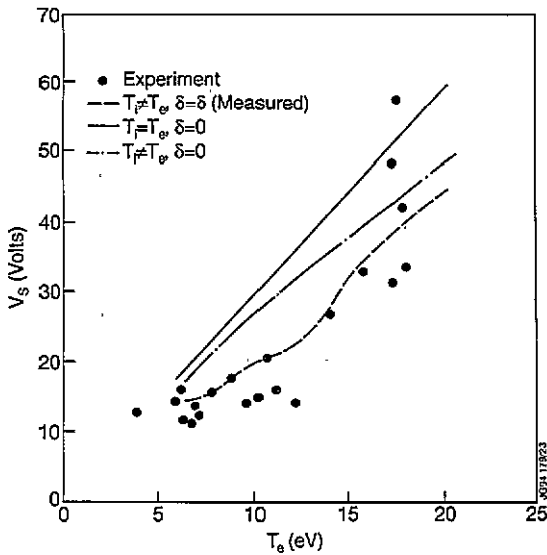


Figure 20. Theoretical and experimental sheath potentials for a surface in ion saturation. Best agreement is obtained when measured ion temperature and ion-induced secondary-electron emission are included.

relies on the principle that near or below the floating potential the current flow to the probe is not restricted by the cross-field mobility of the electrons. Comparisons over a much wider range of conditions would be highly desirable.

Perhaps the most interesting new application of RFAs is for the *in situ* measurement of ion and electron secondary-electron emission yields (Pitts and Matthews 1990). A schematic of the probe used by Pitts is shown in figure 19(a) (Pitts and Matthews 1990). Carbon and molybdenum samples were exposed through a large aperture to condition them and then rotated into position. The bias configuration was then varied so that for a fixed incoming distribution of ions or electrons, the secondary electrons were retained or repelled from the collector material in a cyclical fashion, as shown in figure 19(b). Finally, the formula for the sheath potential was evaluated using measured ion and electron temperatures and secondary electron yields. Figure 20 shows a comparison between this theoretical value and the sheath potential measured in the same experiment (Pitts and Matthews 1990). Unfortunately, this experiment was incomplete in that it was only carried out for a surface biased into ion saturation for which electron-induced secondary electrons would play no part. The measurements of secondary-electron yields indicated that the combined ion and electron secondary-emission yield would be expected to exceed unity for carbon and molybdenum. Conventional sheath theory described by equation (6) is predicted to fail for secondary-electron yields greater than 0.8 (Hobbs and Wesson 1967) so this would be an interesting and important area for further experimental work.

It is also worth noting that the electron-induced secondary-electron emission is not expected to affect the interpretation of Langmuir probe data but that ion-induced secondary electrons will increase the apparent ion flux. On DITE the ion-induced secondary-electron yields were measured in the range $\delta_i = 0.15-0.5$ (Pitts *et al* 1989). This time-dependent variation may well be dependent on the

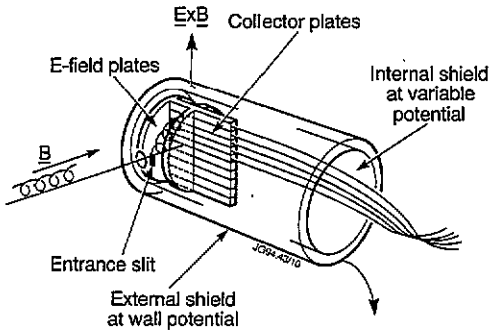


Figure 21. The $E \times B$ probe is a parallel velocity analyser which relies on guiding centre drift in crossed electric and magnetic fields.

charge state mix of the incident ions as well as the surface material. The uncertainty introduced into the ion saturation current of a Langmuir probe is, however, of the same order as many other uncertainties in Langmuir probe interpretation.

3.4. $E \times B$ probes

The principle of the $E \times B$ probe is illustrated in figure 21 (Staib 1982). Ions enter the device parallel to the magnetic field via an aperture slit and pass down the gap between two parallel electrodes which apply an electric field at right angles to B . The guiding centres of the ions all drift normal to E and B with a common velocity E/B . In principle the distribution of parallel velocity is unaffected and so the distribution of current measured at the exit plane is a direct measure of the distribution of parallel velocities. Staib (1980) was the first to apply an electrical probe based on this principle to the diagnosis of the tokamak SOL. Since the collector currents can be measured simultaneously, high time resolution can be achieved; however, energy resolution is seriously limited by the need to make the collectors smaller than the ion gyro-radius. If a collector integrates the ion over distances less than the gyro-radius, the guiding centre approximation, on which the technique is based, is inapplicable.

Figure 22 shows an ion energy distribution from the $E \times B$ probe used in ASDEX (Staib 1982). Although it was not pointed out in that paper, these results are rather surprising because there is apparently significant ion current at low energies. If the plasma sheath were established across the entrance aperture then all ions should have a minimum energy of $\sim 3T_e$. However, as has been demonstrated with the RFA measurements, this can be reduced by secondary-electron emission but not by enough to explain the $E \times B$ probe data. In the case of the ASDEX data this effect may have been caused by the fact that the entrance slit was considerably larger than the Debye length. However, these measurements were repeated on DITE with a sub-Debye length slit and similar puzzling results were found (Mathews 1984b). It is really only since the work with plasma ion mass spectrometers (PIMS) that likely causes of this problem can be identified:

(i) At the time it was a commonly held belief that the impurity concentration in the scrape-off layer was only a few per cent. PIMS measurements described in the next section showed that not only were impurity concentrations higher than this but also that due to the absence of coronal equilibrium, the current delivered to a surface by these ions, due to their high charge states, could equal that due to the

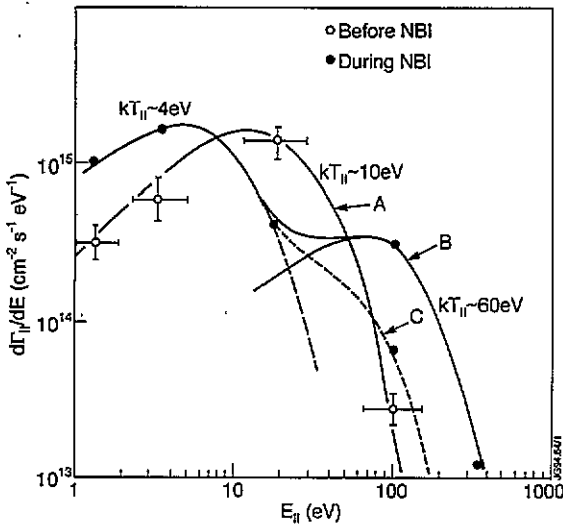


Figure 22. Ion energy distribution from an $E \times B$ probe in ASDEX during the ohmic phase (A) and at the beginning (B) and end (C) of the neutral beam heating pulse (1.2 MW injected into a 320 kA discharge with $\bar{n}_e = (2-4) \times 10^{19} \text{ m}^{-3}$). There appears to be significant flux at very low energies.

majority plasma ions. $E \times B$ probes are essentially velocity analysers and not energy analysers. Ions of equal charge acquire the same energy when crossing the sheath and so the resulting velocity depends on the square root of the mass. Impurities may therefore have contributed to currents seen on the low-energy collectors.

(ii) The second effect which may have contributed is that the assumption that on entering the probe the ions immediately experience an electric field at right angles to the magnetic field is also flawed. In fact, significant defocusing occurs which mixes parallel and perpendicular velocity. This has been observed in the cycloidal focusing PIMS and in this case is generally beneficial (Matthews *et al* 1990b).

This story provides two lessons. First—it is never safe to assume that impurities can be ignored in the tokamak edge. Second—attention to detail is essential when designing ion optical systems, without this a blurred image of the source distribution may result. Despite these problems $E \times B$ probes can give sensible results as can be seen from the comparison between the RFA and $E \times B$ measurements of ion temperature shown in figure 23 (Matthews 1984a). Sheath voltage is much more problematical and there is no experimental evidence that $E \times B$ probes can yield believable values of this parameter.

3.5. Mass spectrometers

On the basis of a coronal model one would expect the charge state distribution to be characteristic of the relatively low SOL electron temperature. However, ions diffuse out of the hotter regions of the plasma into the edge and have a low probability of recombination. Impurities in the edge plasma are therefore highly non-coronal. The charge state mix of impurities arriving at the limiters or divertor target plates is thus a complex function of geometry, plasma parameters and transport not just locally but for the *whole* machine. For example, the flux of fully stripped ions into the SOL

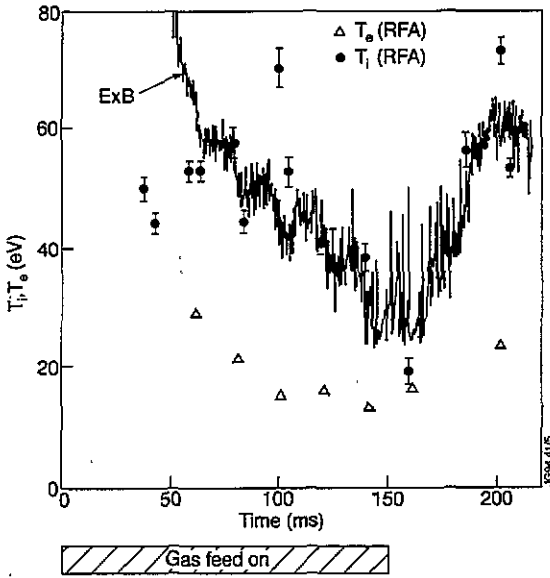


Figure 23. Comparison of $E \times B$ and RFA measurements of ion temperature in DITE.

is a function of the core plasma temperature and density profiles and the rate at which lower charge states diffuse into the hotter regions. The flux of low-charge-state ions on the other hand depends only on local plasma conditions and transport. There is therefore a lot of useful information locked up in the charge-state distribution of the impurities over and above the question of how much sputtering it will cause at a surface. On a more basic level we may wish to know the total concentration of each impurity in the SOL since this can give a clear indication as to the primary source.

It has been obvious for a long time that the mass spectrometer has had enormous potential as a plasma diagnostic (Osher 1965). But it has taken a very long time for such a device to be successfully implemented in the edge of a tokamak. Clearly any mass spectrometer design has to take account of the large magnetic field which confines the tokamak plasma. Historically, the favourite device has been the 180° mass spectrometer which offers a simple geometry but rather poor velocity focusing (Kojima *et al* 1984). In contrast the cycloidal focusing mass spectrometer which employs crossed electric and magnetic fields offers perfect focusing of perpendicular velocity components (Bleakney and Hipple 1938) and is as yet the only device to be successfully applied to the SOL of a large tokamak. The omegatron mass spectrometer uses an oscillating electric field which is resonant with the cyclotron frequency of a particular ion (Sommer *et al* 1951). Although not yet proven in a tokamak, an omegatron has worked successfully in the PISCES linear plasma device (Wang *et al* 1990) and a probe head is being developed for C-Mod (Thomas 1993). The basic geometry of the three mass spectrometers is illustrated in figure 24 with examples of mass spectra from each type. The 180° and omegatron mass spectrometers have inherent rejection of M/Z harmonics (e.g. 2, 4, 8 etc) and the cycloidal focusing PIMS also removes harmonics provided that the geometry is carefully chosen (Matthews 1989).

The 180° mass spectrometer has only ever been used in the SOL of an extremely

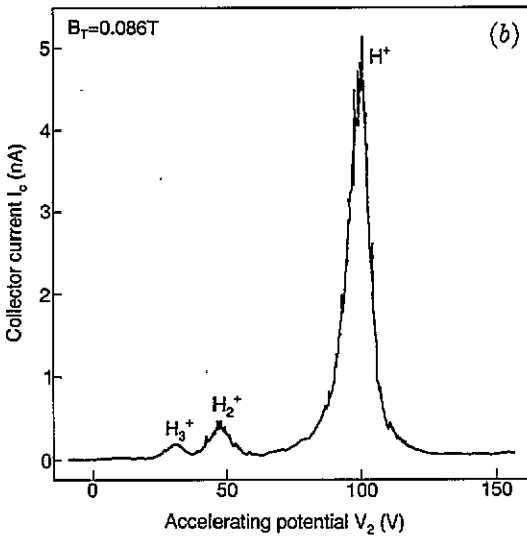
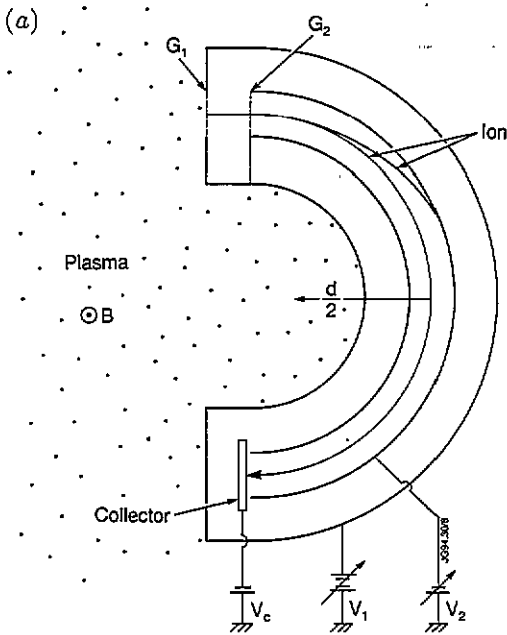


Figure 24. The three plasma ion mass spectrometer (PIMS) types which have been used or designed for use in the tokamak SOL. (a) 180° PIMS with measurements from a very small high-frequency tokamak (b) (Kojima *et al* 1984). Cycloidal focusing PIMS (c), with a spectrum taken in the DITE tokamak in a hydrogen plasma (d) (Matthews *et al* 1990b). Omegatron PIMS (e) designed for use in Alcator C-Mod with test data from a linear plasma machine with hollow cathode source (f) (Thomas 1993).

small tokamak (Kojima *et al* 1984) and in the divertor of a stellarator (Gibson *et al* 1964). Unfortunately, because tokamak SOL plasmas are hot ion sources the velocity focusing of the 180° instrument makes both the transmission and resolution sensitive to the ion energy distribution (Kojima *et al* 1984). Also the geometry of the device does not allow one to extract ions from the plasma in a well defined way. The natural method is to allow ions to enter the device across the magnetic field. Unfortunately, this process seems to be fraught with uncertainties in that the transmission probability will depend on the electric field structure in front of the slit

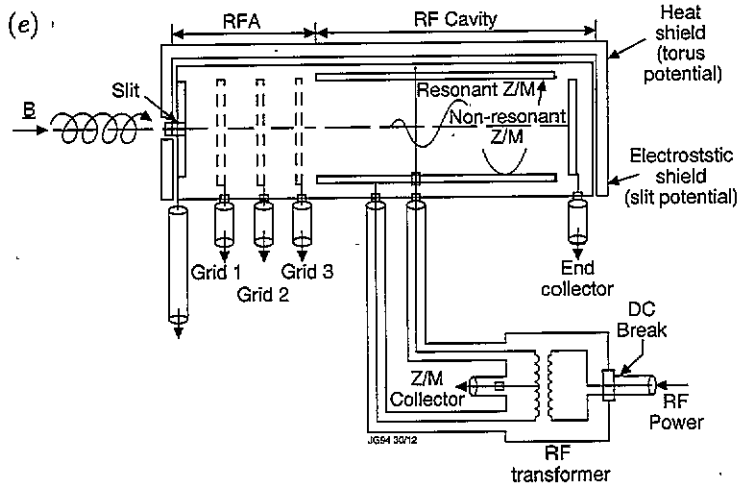
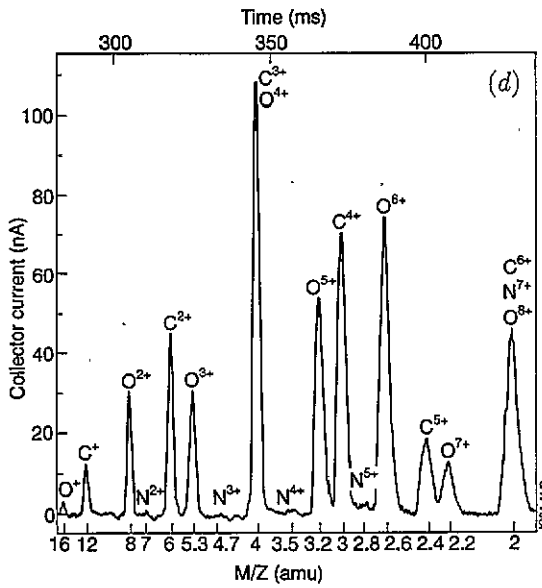
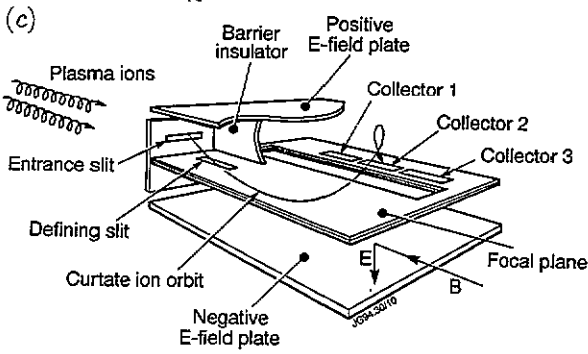


Figure 24. (Continued)

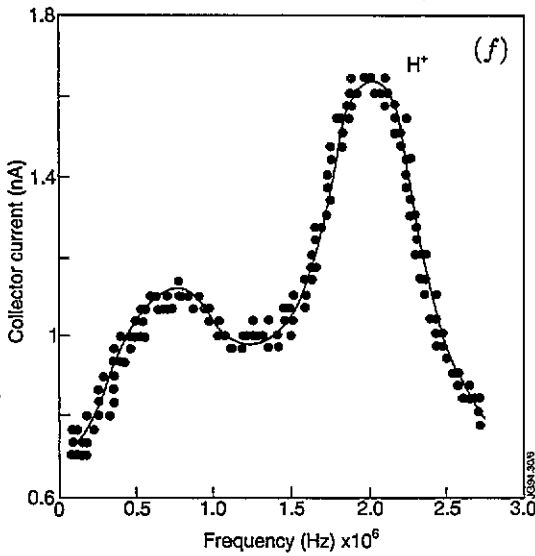


Figure 24. (Continued)

and the gyro-radius of each species of ion. Since it is very hard to see how such devices can be calibrated, such a large uncertainty in the probability of transmission is highly undesirable.

In the case of the cycloidal focusing mass spectrometer or omegatron, ions can flow into the device along the magnetic field, thus making a clean transition from the plasma to the mass spectrometer. The focusing properties of both these instruments are also independent of perpendicular ion energy. The main justification for developing the omegatron is that the focal length of the cycloidal focusing PIMS is proportional to E/B^2 . Experience shows that the breakdown voltage is limited in these devices to around 2 kV and that this is more or less independent of size. Combining this with the fact that the electric field plates must be given a separation which is a constant multiple of the gyro-radius, the focal length of cycloidal focusing device scales as $1/B$. The cycloidal focusing instruments applied to DITE (Matthews *et al* 1990b) and TEXTOR (Matthews *et al* 1992b) had a focal length of 9 mm and were able to measure $M/Z = 2$ to ∞ at toroidal fields up to a limit of 2.25 T. Scaling this to the 6 T toroidal field expected at the probe location in Alcator C-Mod, the required focal length is ~ 3.4 mm. Although it is quite possible that a device of this size could be fabricated, it would not be easy. The omegatron on the other hand has a much simpler construction and can be constructed using conventional techniques. In theory, high mass resolution is also simpler to achieve in an omegatron than in a cycloidal PIMS. However, the omegatron has the disadvantage that the electronics are more complicated since a swept RF source up to 92 MHz is required if H^+ ions are to be studied.

Finally, it is worth noting that all the mass spectrometers discussed are really M/Z spectrometers and so overlaps inevitably occur (e.g. He^+ , C^{3+} , O^{4+} , ${}_{20}Ne^{5+}$ at $M/Z = 4$). In some cases these clashes can be removed using known isotope ratios. In Textor for example, neon injection experiments were carried out in which it was possible to deduce the flux of ${}_{20}Ne^{5+}$ from the unobscured ${}_{22}Ne^{5+}$ peak given that the natural abundance of ${}_{22}Ne$ is 8.82%. Unfortunately, in this experiment the

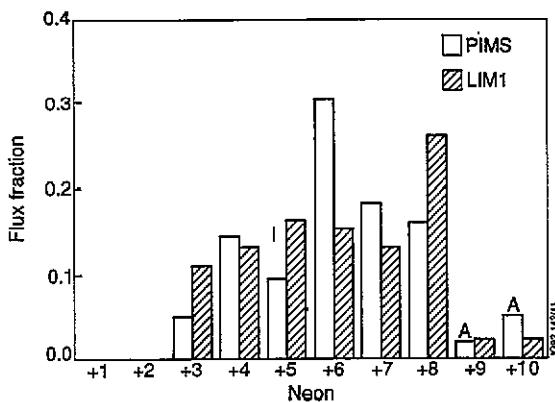


Figure 25. Comparison of the charge state distribution of neon ions in the SOL of TEXTOR compared with the predictions of the LIM Monte Carlo impurity transport code. Ambiguous charge states are marked with an A and were resolved with a variety of rules (see text). The charge state marked I was resolved using a known isotope ratio.

hydrogen-like and fully stripped neon ions were ambiguous and the fluxes were guessed by assuming that the ratio between the fluxes of these ions and that of the known helium-like state was the same as had been measured for $_{11}\text{B}$ which were resolved (see figure 24(b)). Comparison with the predictions of the Monte Carlo impurity transport code LIM indicates that this approach can be satisfactory, as shown in figure 25 (Matthews *et al* 1992b).

3.5.1. Impurity ion energy. In a conventional mass spectrometer the time it takes an ion to travel from the source to the collector is not that important, but for a PIMS it is crucial. This is because none of the mass spectrometer designs focus ion velocity components which are parallel to the magnetic field. In a conventional mass spectrometer with a cold internally generated ion source this is not a problem because ion energies are negligible and ions can in some cases be trapped in a potential well. With a PIMS the source of ions is external and hot, so the combination of thermal energy and acceleration in the plasma sheath means that ions entering the analysis region have substantial parallel velocities.

The 180° mass spectrometer focuses ions in half a gyro-period and the cycloidal PIMS in one gyro-period. Interestingly, ions in an omegatron reach the collector in a time independent of M/Z (Thomas 1993). If R_0 is the radius of the collector, B the magnetic field strength and E_0 the amplitude of the RF electric field then the time to collection is $t_c = 2R_0B/E_0$. It is clearly important to ensure that the time it takes ions to drift out of the far end of the device is longer than t_c . In the omegatron device planned for C-Mod this is feature is made use of by biasing the RF cavity so as to reduce the parallel energy of incoming ions. This is very similar to the retarding field analyser method but provides the means to energy analyse an individual impurity charge state and has been proven to work in a linear plasma machine at a magnetic field of 0.14 T (Thomas 1993).

Although the RFA approach could also be applied to the cycloidal focusing PIMS, the only method proven so far is to use the dispersion of current on a series of collectors lying parallel to the field. Reasonable agreement was obtained between ion temperatures obtained with an RFA (assuming $M/Z = 2$ to correct for mean

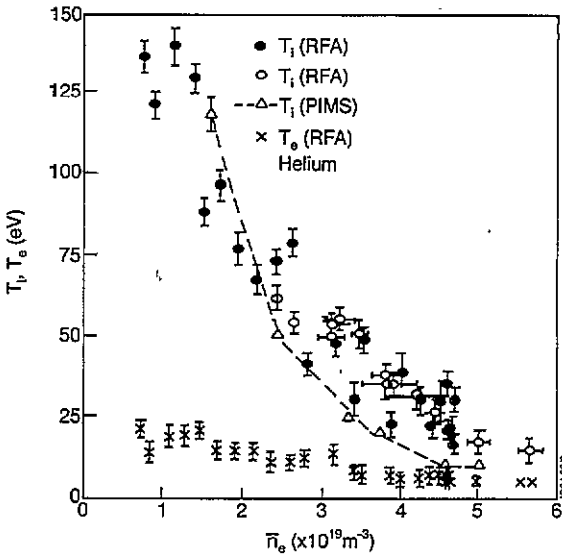


Figure 26. Variation of edge ion temperature with line-averaged density in DITE measured with RFA and PIMS.

charge state) and those obtained with the cycloidal focusing PIMS (no assumption about M/Z required). The results are shown in figure 26 (Matthews *et al* 1990b). This method did not, however, offer sufficient resolution to allow independent determination of the ion temperatures of individual charge states, although it was only the first two charge states which were expected to have significantly lower temperatures. One important subtlety of the cycloidal PIMS temperature measurement is that it proves to be mainly a measurement of perpendicular ion temperature. This is a consequence of an unintentional electrostatic lens at the point where ions enter the device (Matthews *et al* 1990b).

4. Conclusions

Langmuir probes have for a long time been the most popular diagnostic for diagnosing tokamak edge plasmas. This has resulted from the relative simplicity of the method and the spatially localized nature of the measurements. Although some have predicted that non-perturbing spectroscopic methods would render electrical probes obsolete, there is still no sign of this happening. The development of limiter and divertor probe arrays and fast-moving probe drives has made electrical probes relevant for even the largest tokamaks in operation today. However, these developments have introduced problems. Flush-mounted Langmuir probes designed to withstand high power loads have experienced non-saturation of the ion current and low electron to ion-saturation current ratios which have made interpretation difficult. Progress is being made on understanding these effects but there is still a long way to go.

Studies of impurity retention in diverted tokamaks are making measurements of SOL flow velocities of great interest, since the frictional terms are thought to play an important role in the force balance acting on impurity ions. Mach probes have an

important role to play here and there has been important progress in the theory which is applied to the interpretation of these probes.

Divertor impurity retention is also thought to depend very strongly on the SOL ion temperature. Ion energy analyser probes have been proven to provide the required diagnostic capability. Retarding field analysers have proven particularly versatile and can provide additional information about the sheath voltage and even the secondary-electron emission yields for ions and electrons. Combining all this information, quite detailed studies of the physics of the sheath are possible but still have to be fully exploited. Fast probe drives should even make this technique practical in large high-power tokamaks.

Impurities can themselves be directly measured with *in situ* plasma ion mass spectrometry (PIMS). Measurements in TEXTOR and DITE, using a cycloidal focusing PIMS, have provided by far the most comprehensive quantitative inventory of the fluxes of impurity and fuel ions across the full range of charge states yet achieved by any method. Measurement of impurity ion temperature was also demonstrated. A simpler omegatron-based PIMS has also recently been developed, which it is hoped will prove applicable to the SOL of high-field tokamaks.

There is still enormous potential for the development and application of all types of electrical probes. It is important that this is done because taken as whole electrical probes have the capability to tell us almost all we would like to know about tokamak edge plasmas. Problems of interpretation remain, but in general we know how to avoid them and there is still steady progress in probe theory.

References

- Armstrong R J, Liland K-B and Trulsen J 1992 *Physica D* **60** 160-4
 Asakura N *et al* 1993 *APS Conf. (St Louis)* poster 2R8
 Behringer K 1987 *J. Nucl. Mater.* **145-147** 145
 Bergmann A 1993 *20th EPS Conf. on Controlled Fusion and Plasma Physics (Lisbon)* (European Physical Society) vol 17C II p 803
 Bleakney W and Hipple J A 1938 *Phys. Rev.* **53** 521
 Budny R and Manos D 1984 *J. Nucl. Mater.* **121** 41
 Carlson A *et al* 1993 *20th EPS Conf. on Controlled Fusion and Plasma Physics (Lisbon)* (European Physical Society) vol 17C III-1103
 Chung K-S and Hutchinson I H 1988 *Phys. Rev. A* **38** 4721
 — 1989 *Phys. Fluids B* **1** 2229
 Chung K-S 1993 *Nucl. Fusion* submitted
 Cohen S A 1978 *J. Nucl. Mater.* **76&77** 68
 Cuthbertson J W, Buchenauer D A, Hill D N, Futch A H and Maingi R 1992 *APS Conf. (Seattle)*
 El Shaer M 1981 *These de Docteur—Ingenieur* Universite Scientifique et Medicale de Grenoble
 Erents S K *et al* 1989 *J. Nucl. Mater.* **162-164** 226-30
 Futch A H *et al* 1992 *J. Nucl. Mater.* **196-198** 860-4
 Gibson A, Bishop A S, Hinnov E and Hofmann F W 1964 *MATT Report 261* (Plasma Physics Laboratory, Princeton University)
 Gunther K, Herrmann A, Laux M, Pech P and Reiner H-D 1990 *J. Nucl. Mater.* **176-177** 236
 Hershkowitz N 1989 *Plasma Diagnostics Volume 1, Discharge Parameters and Chemistry* ed O Auciello and D L Flamm (Boston: Academic) pp 113-83
 Hobbs G D and Wesson J A 1967 *Plasma Phys.* **9** 85
 Hutchinson I H 1987 *Phys. Fluids* **30** 3777
 — 1988 *Phys. Rev. A* **37** 4358
 — 1991 *Phys. Fluids B* **3** 847
 Katsumata I and Okazaki M 1967 *Japan J. Appl. Phys.* **6** 123

- Keilhacker M *et al* 1990 *Plasma Physics and Controlled Nuclear Fusion Research IAEA-CN-53/A-V-1* (Vienna: IAEA) pp 345–64
- Kojima H, Sugari H, Mori T, Toyada H and Okuda T 1984 *J. Nucl. Mater.* **128–129** 965
- Labombard B, Lipshultz B and Jablonski D 1993 *APS Conf. (St Louis)* poster 386
- Labombard B *et al* 1989 *J. Nucl. Mater.* **162–164** 314
- Maclatchy C S *et al* 1992 *J. Nucl. Mater.* **196–198** 248–52
- Maddison G P, Reiter D, Stangeby P C and Prinja A K 1993 *20th EPS Conf. on Plasma Physics and Controlled fusion* (Lisbon) (European Physical Society) Vol 17C pt II p 803
- Manos D M, Budney R, Satake T and Cohen S A 1982 *J. Nucl. Mater.* **111–112** 130
- Manos D M and McCracken G M 1986 *Physics of Plasma–Wall Interactions in Controlled Fusion Devices (NATO ASI Series B: Physics 131)* (New York: Plenum) pp 135
- Matthews G F 1984a *DPhil Thesis* University of Oxford
- 1984b *J. Phys. D: Appl. Phys.* **17** 2243–54
- 1989 *Plasma Phys. Control. Fusion* **31** 841–53
- Matthews G F, Fielding S J, McCracken G M, Pitcher C S, Stangeby P C and Ulrickson M 1990a *Plasma Phys. Control. Fusion* **32** 1301–20
- Matthews G F, Hill D N and Ali Mahdavi M A 1991b *Nucl. Fusion* **31** 1383–5
- Matthews G F, Pedgeley J M, Pitts R A and Stangeby P C 1990b *J. Nucl. Mater.* **176–177** 1032
- Matthews G F, Pitts R A, McCracken G M and Stangeby P C 1991a *Nucl. Fusion* **31** 1495–509
- Matthews G F *et al* 1992a *J. Nucl. Mater.* **196–198** 374–9
- Matthews G F *et al* 1992b *J. Nucl. Mater.* **196–198** 253–7
- McCracken G M *et al* 1990 *J. Nucl. Mater.* **176–177** 191
- Osher J E 1965 *Plasma Diagnostic Techniques* ed R Huddleston and S Leonard p 519
- Pitcher C S *et al* 1993 *20th EPS Conf. on Controlled Fusion and Plasma Physics (Lisbon)* (European Physical Society) vol 17C pt I p 73
- Pitts R A 1991a *PhD Thesis* University of London
- 1991b *Phys. Fluids B* **3** 2871
- Pitts R A and Matthews G F 1990 *J. Nucl. Mater.* **176–177** 877–82
- Pitts R A, Matthews G F and McCracken G M 1989 *J. Nucl. Mater.* **162–164** 568
- Proudfoot G, Harbour P J, Allen J and Lewis A 1984 *J. Nucl. Material* **128–129** 180
- Roth J 1986 *Physics of Plasmas–Wall Interactions in Controlled Fusion Devices (NATO ASI Series B Physics 131)* (New York: Plenum) p 351
- Schorn R P *et al* 1991 *Appl. Phys. B* **52** 71–8
- Schorn R P *et al* 1992 *Nucl. Fusion* **32** 351–9
- Sofield C J *et al* 1981 *Nucl. Instrum. Methods* **191** 383
- Sommer H, Thomas H A and Hipple J A 1951 *Phys. Rev.* **82** 697
- Staib P 1980 *J. Nucl. Mater.* **93 & 94** 351
- 1982 *J. Nucl. Mater.* **111 & 112** 109–22
- Stamp M F and Summers H P 1990 *Controlled Fusion and Plasma Heating (Proc. 17th European Conf. Amsterdam, 1990)* vol 14B pt III (European Physical Society) p955
- Stangeby P C 1982 *J. Phys. D: Appl. Phys.* **15** 1007
- 1984a *Phys. Fluids* **27** 2699
- 1984b *J. Nucl. Mater.* **128 & 129** 969–73
- 1986 *Physics of Plasma–Wall Interactions in Controlled Fusion Devices (NATO ASI Series B Physics 131)* (New York: Plenum) p 41
- 1989 *Plasma Diagnostics Volume 2, Surface Analysis and Interactions* ed O Auciello and D L Flamm (Boston: Academic) p 157–209
- Stangeby P C, Farrell C, Hoskins S and Wood L 1988 *Nucl. Fusion*, **28** 1945
- Stangeby P C and McCracken G M 1990 *Nucl. Fusion* **30** 1225
- Stangeby P C Pitcher C S and Elder J D 1992b *Nucl. Fusion* **32** 2079–89
- Stangeby P C *et al* 1992a *J. Nucl. Mater.* **196–198** 374
- Staudenmaier P, Staib P and Poschenrieder W 1980 *J. Nucl. Mater.* **93 & 94** 121
- Tagle J A, Stangeby P C and Erents S K 1987 *Plasma Phys. Control. Fusion* **29** 297
- Thomas E E 1993 *MIT Plasma Fusion Center Report PFC/RR-93-03*
- Thomas E W 1984 *Data Compendium for Plasma Surface Interactions (Nucl. Fusion Special Issue)* **94**
- Vlases G C and the JET Team 1992 *14 IAEA Conf. Wurzburg IAEA-CN-56/A-5-1* (Vienna: IAEA)
- Von Hellermann M G and Summers H P 1993 *JET Preprint JET-P(93)34*
- Wang E Y *et al* 1990 *Rev. Sci. Instrum.* **61** 2155